ORIGINAL PAPER

Hee-Jin Ryoo · Hee-Tak Kim · Young-Gi Lee
Jung-Ki Park · Seong-In Moon

Thermal and electrochemical characteristics of plasticized polymer electrolytes based on poly(acrylonitrile-*co*-methyl methacrylate)

Abstract The thermal and electrochemical characteristics of plasticized polymer electrolytes composed of poly(acrylonitrile-*co*-methyl methacrylate) [P(AN-*co*-MMA)], a plasticizer [a mixture of ethylene carbonate and propylene carbonate], and $LiCF_3SO_3$ were investigated. The incorporation of a MMA unit into the matrix polymer was effective for an increase in the compatibility between the matrix polymer and the plasticizer. The comparative investigation of the interfacial resistance of the Li/polymer electrolyte/Li cell for the PAN-based and the P(AN-*co*-MMA)-based polymer electrolytes showed that the MMA unit could improve the stability of the polymer electrolyte toward the Li electrode, which is probably due to the enhanced adhesion of the polymer electrolyte to the Li electrode.

Key words Plasticized polymer electrolyte ·
Poly(acrylonitrile-*co*-methyl methacrylate) · Ionic
conduction · Passivation · Lithium polymer battery

Introduction

Plasticized polymer electrolytes in which liquid electrolyte is immobilized by incorporation into a matrix polymer have been proved to be most promising for the electrolyte system used in lithium polymer batteries (LPB) owing to their high ionic conductivities [1–13]. However, there is still a need of improving the stability of the plasticized polymer electrolytes toward the lithium electrode in terms of cyclability and safety [14–16].

H.J. Ryoo · H.T. Kim · Y.G. Lee · J.K. Park (✉)
Department of Chemical Engineering,
Korea Advanced Institute of Science and Technology,
373-1, Kusung-dong, Yusung-gu, Daejon, 305-701, Korea

S.I. Moon
Battery Technology Team,
Korea Electrothechnology Research Institute,
Changwon, 641-600, Korea

Various kinds of polymers have been considered as a matrix polymer for plasticized polymer electrolytes. Among them, polyacrylonitrile (PAN) has received special attention due to the high ionic conductivity and the exceptionally good mechanical strength of the corresponding polymer electrolytes. However, these favorable properties are somewhat contrasted by the poor compatibility of the PAN-based polymer electrolyte toward the lithium electrode, causing serious passivation [1, 17, 18].

From a qualitative point of view, poly(methyl methacrylate) (PMMA)-based electrolytes showed more stable interfacial resistance under prolonged storage compared with the PAN-based polymer electrolytes [19]. This behavior is probably associated with the good miscibility of PMMA with the plasticizer. Hence, the incorporation of a small amount of methyl methacrylate into the polyacrylonitrile chain could be a reasonable way of improving the interfacial stability of the PAN-based polymer electrolytes. The present article reports the thermal and electrochemical characteristics of the polymer electrolytes based on [P(AN-*co*-MMA)]. The miscibility of the copolymer with the plasticizer was examined from the melting and the recrystallization behavior of the plasticizer, EC, in the polymer electrolytes. The effect of the MMA unit introduced into the polyacrylonitrile chain on the ionic conduction of the polymer electrolytes and the interfacial resistance of the Li/polymer electrolyte/Li cell was also investigated.

Experimental

Synthesis of poly(AN-*co*-MMA)

Acrylonitrile and methyl methacrylate were purchased from Aldrich and used as received. The redox initiators, potassium persulfate ($K_2S_2O_8$) and sodium bisulfite ($NaHSO_3$), were also purchased from Aldrich and used after drying in vacuum at 120 °C for 48 h.

In order to copolymerize AN and MMA monomer, the initiators, $K_2S_2O_8$ and $NaHSO_3$, were added to a 10 wt% water solution of the mixture of the AN and MMA monomers. The molar ratio of

the initiator to the monomers was set to be 0.005 for $K_2S_2O_8$ and 0.0025 for $NaHSO_3$. The reactions were conducted at room temperature under nitrogen atmosphere. As the copolymerization proceeded, the reacting medium changed to a white suspension and minute particles were produced. The precipitated particles were filtered and washed twice with distilled water at 80 °C to remove any impurities such as the residual initiators. The filtered product was kept in a hood at room temperature for 24 h, and then dried under vacuum at 80 °C for 48 h to remove any trace of water in the product.

Gel permeation chromatography measurements

The molecular weight of the copolymers was determined by a gel permeation chromatograph (GPC) equipped with four Shodex-KD columns (500 Å, 10^3 Å, 10^4 Å, 10^5 Å) at a flow rate of 1.0 ml/min operated at 50 °C. The 10 wt% DMF solutions of the copolymers were filtered before they were injected into the GPC apparatus. The system was calibrated with the polystyrene standard using DMF as eluent.

Differential scanning calorimetry measurements

Differential scanning calorimetry (DSC) experiments were carried out at a heating rate of 10 °C/min by using the DuPont 910 differential scanning calorimeter. Samples were loaded in hermetically sealed cells and measurements were always carried out under dry nitrogen atmosphere.

Preparation of polymer electrolytes

The copolymer and the salt ($LiCF_3SO_3$) were mixed with the mixture of ethylene carbonate (EC) and propylene carbonate(PC) in a closed bottle at 110 °C to prepare a 10 wt% homogeneous polymer solution. The amount of the salt was adjusted to be 7 wt% based on the total amount of the plasticizer. The hot solution was cast on a Teflon molder and then dried at 60 °C to evaporate the plasticizer slowly. After evaporation of the appropriate amount of plasticizer, the films were separated from the Teflon molder. The thickness of the films were in the range 450–650 μm.

Scanning electron microscopy measurements

The morphology of the polymer electrolyte films were investigated by scanning electron microscopy (SEM) using the Philips SEM 535M. The accelerating voltage and tilt angle were 30 kV and 30°, respectively. The plasticizer in the specimen was removed by freeze drying without any change in the morphology of the specimen. Since the scanning electron microscope is operated under vacuum, removal of the plasticizer is needed. After being quenched in liquid nitrogen for 30 min, the films were mounted in freeze dryer equipment and dried under a reduced pressure of 100 mmHg for 12 h. The specimens for the SEM images of the cross section of the films were prepared by fracturing the corresponding films in liquid nitrogen.

Electrical measurements

The specimen for ionic conductivity measurement was prepared by sandwiching the polymer electrolyte between two stainless steel electrodes of which the diameter was equal to 13 mm. The impedance of the specimen was taken over the frequency range of 10–10 MHz using the Solatron 1255 frequency response analyzer. The data were transmitted from the frequency response analyzer to the personal computer through GPIB. The conductivity was obtained from the bulk resistance found in the complex impedance diagram.

In order to measure the interfacial resistance of the Li/polymer electrolyte/Li cell, a square of polymer electrolyte film of 4 cm² size was sandwiched between the two lithium electrodes. The sandwich was vacuum-packed in an aluminized polyethylene bag (Blue Bag) in order to avoid its contamination by humidity. The a.c. impedance was regularly measured during storage at room temperature.

Results and discussion

Structural characterization of the P(AN-co-MMA)

Copolymers with the molar content of the acrylonitrile unit varying from 76 to 100 mol% were synthesized. ^{1}H NMR analysis was used to determine the compositions of the copolymers. Figure 1 shows the ^{1}H NMR spectra of the copolymers. The peak at 2.07–2.18 ppm was assigned to the methylene (CH_2) protons in the MMA unit and the peaks ranging from 1.06 to 1.40 ppm correspond to the α-methyl (CH_3) protons in the MMA unit. Since the methyl protons linked to the adjacent carbonyl group in the MMA unit donate electrons to the oxygen in the carbonyl group, their peaks shifted downfield and appeared at 3.63–3.71 ppm. The methine proton peak in the AN unit appeared at 3.15–3.2 ppm [20, 21].

As listed in Table 1, $\bar{M}_n$, $\bar{M}_w$, and the polydispersity of the copolymers were $1.6–2.2 \times 10^5$, $4.6–8.2 \times 10^5$, and 2.7–3.7, respectively. The glass transition temperatures of the copolymers were in the range 95–100 °C.

For brevity, the copolymers will be designated in this paper as ANn, where n indicates the mol% of the AN unit in the copolymer [AN93, for example, means poly(AN-co-MMA) with AN content of 93%].

Mechanical state of the prepared polymer electrolytes

The mechanical state of the polymer electrolyte films was found to change considerably with the composition
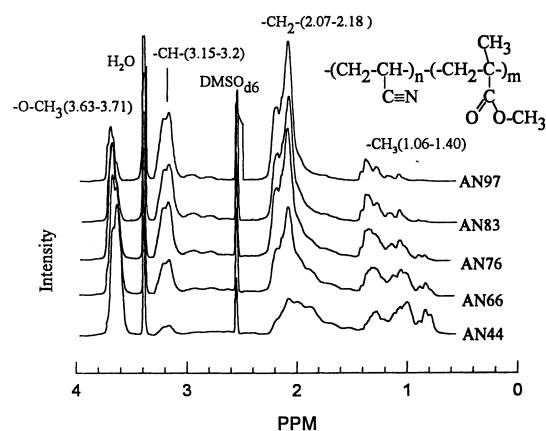

Fig. 1 ^{1}H NMR spectra of P(AN-co-MMA)s (solvent: DMSO-d_o, reference: TMS)

Table 1 Molecular weights and glass transition temperatures of P(AN-co-MMA) copolymers

Copolymer	AN (mol%)	$\bar{M}_n$	$\bar{M}_w$	PDI ($\bar{M}_w/\bar{M}_n$)	T_g (°C)
AN76	76	163 000	500 000	6.0	95
AN83	83	170 000	560 000	3.4	95
AN89	89	190 000	690 000	3.6	96
An97	97	222 000	830 000	3.7	100

Table 2 Mechanical state of the P(AN-co-MMA)-based polymer electrolytes

Plasticizer content (wt%)[a]	Host polymer[b]				
	PAN	AN97	AN89	AN83	AN76
200	FR	FF	FF	FF	FF
250	FR	FF	FF	FF	FF
300	FR	FF	FF	FF	FS
350	FR	FF	FF	FF	G
400	FR	FF	FS	FS	G

[a] Plasticizer content $= 100 \times$ [wt. of plasticizer]/[wt. of polymer]
[b] FR, free standing and rigid; FF, free standing and flexible; FS, free standing and sticky; G, gel

of the matrix copolymer and the plasticizer content. The stiffness of the film increased with an increase of the AN content in the matrix copolymer. Table 2 summarizes the mechanical state of the various polymer electrolytes prepared in this study. The difference in the mechanical state of these polymer electrolytes could be reasonably explained in terms of the compatibility between the copolymer and the plasticizer. Owing to the poor miscibility between the AN unit and the plasticizer, the plasticizer and the polymer would be phase-separated in the polymer electrolytes based on the copolymers with a high AN content, and thus the polymer-rich phase could mechanically support the polymer electrolyte film. On increasing the MMA content in the copolymer, the compatibility between the copolymer and the plasticizer enhances, which gives rise to a gel-like structure at a high plasticizer content. The compatibility between the matrix polymer and the plasticizer will be discussed in the following sections.

The polymer electrolyte films based on PAN and AN97 were transparent, whereas those based on AN89, AN83, and AN76 showed a milky appearance, evidencing their phase-separated morphology. In spite of their transparency, the PAN-based polymer electrolytes also revealed microphase-separated morphology, as shown in their SEM images (Fig. 2). The submicron-sized pore shown in the SEM image corresponds to the site where the plasticizer had been filled prior to the removal of the plasticizer by freeze drying. Because the size of the plasticizer-rich phase is too small to scatter light effectively, the PAN-based polymer electrolyte films appear transparent.

Thermal characterization of the polymer electrolytes

In order to obtain information on the interaction between the host polymer and the plasticizer, the physical state of the plasticizer in the polymer electrolytes was
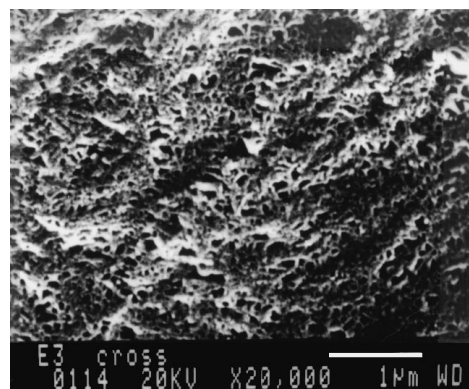

Fig. 2 SEM photograph of the cross section of the PAN-based polymer electrolyte

examined from the melting and recrystallization behavior of the plasticizer. It is expected that the stronger interaction between the plasticizer and the matrix polymer affects the melting and crystallization of the plasticizer to a large extent.

The DSC results for pure EC, the mixtures of EC and PC (EC/PC = 8/2 and 6/4), and the electrolytes based on the copolymers are shown in Fig. 3. In the DSC thermograms of the liquid electrolytes, the melting endotherms, which are originated from the crystal of the plasticizer [22], were clearly recognized irrespective of the composition of the plasticizer, and the melting temperature decreased with the increase of the PC content in the mixture. In addition, the recrystallization peak appeared for the EC/PC (60/40) mixture, whereas it did not for pure EC or the EC/PC (80/20) mixture. The melting behavior and recrystallization behavior indicate that PC interferes with the crystallization of EC.

In the DSC thermograms of the PAN-based and the AN83-based polymer electrolytes (see Fig. 3b and c), the melting endotherms were also observed. These are
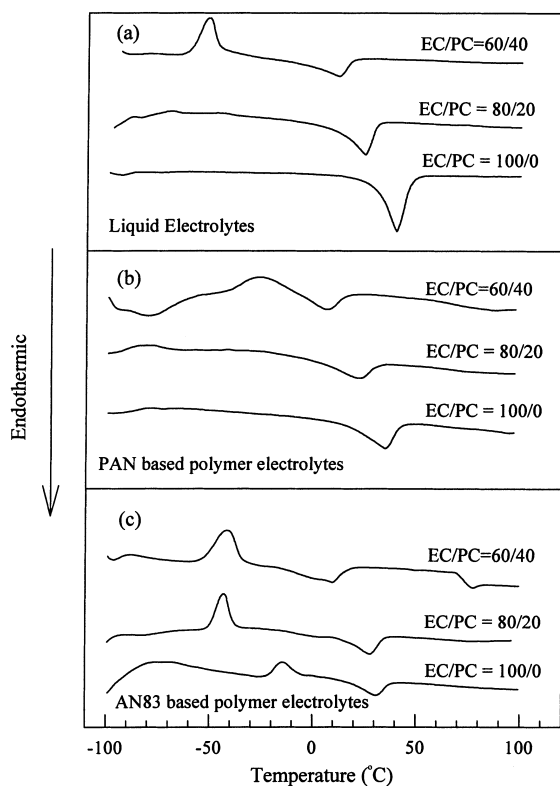
Fig. 3 DSC thermograms of **a** the liquid electrolytes, **b** the PAN-based polymer electrolytes, **c** the AN83-based polymer electrolytes

Fig. 4 X-ray diffraction patterns of **a** the PAN-based polymer electrolytes (plasticizer content: 400%), **b** the AN83-based polymer electrolytes (plasticizer content: 400%)

attributed to the melting of the EC. As shown in the X-ray diffraction patterns (Fig. 4), the peaks from the EC crystal disappeared above the melting temperature for both the PAN-based and the AN83-based polymer electrolytes. One thing to be stressed here is that the melting temperature of the EC crystal was found to be in the following order: liquid electrolyte > the PAN-based electrolyte > the AN83-based electrolyte. This fact implies that the polymer chains cause the imperfection of the EC crystal and this effect is more significant for AN83 compared with PAN. It is indicative of the better miscibility of AN83 with the plasticizer that PAN.

As is shown in Fig. 3, the PAN-based polymer electrolyte and the liquid electrolyte do not show a recrystallization peak during heating when only EC was used as the plasticizer. However, the AN83-based polymer electrolyte containing pure EC clearly shows the recrystallization peak. The appearance of the recrystallization peak, which is caused by suppression of the crystallization of EC, reconfirms the enhancement of the interaction of the host polymer with the plasticizer by incorporation of the MMA unit. The similarity in recrystallization behavior and also in the values of the melting temperatures between the PAN-based polymer electrolyte and the liquid electrolyte could imply a similarity in their physical states. It supports the idea that the microchannel which is occupied by the liquid elec-
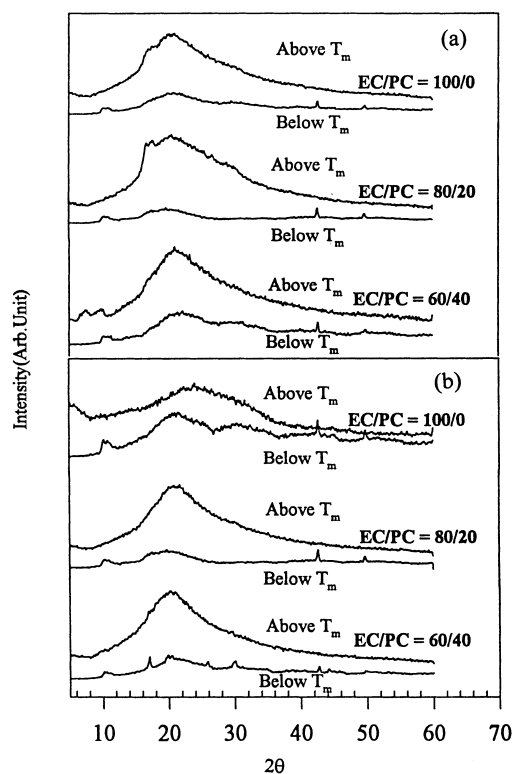
trolyte exists in the PAN-based polymer electrolyte, although the size of the microchannel is too small to be observed by direct observation, i.e., by optical clarity of the film.

Effect of MMA unit in the copolymer on ionic conductivity

Figure 5 shows the temperature dependency of the ionic conductivities of the polymer electrolytes prepared with various copolymers. All the polymer electrolytes considered in this study contained 400 wt% plasticizer (EC/PC = 6/4) based on the weight of the host polymer. An increase of the ionic conductivities with temperature was found, together with an abrupt change in the temperature range 0–10 °C for all the polymer electrolytes. Such behavior had been previously reported by our group in a study of the polymer electrolytes based on poly(methyl methacrylate-co-alkali metal methacrylate) [22]. We have explained this behavior by the melting of the EC crystal in the polymer electrolytes. The change of the ionic conductivity at 0–10 °C was more significant for the PAN-based polymer electrolytes than the copolymer-based electrolytes. Since the crystallization of the plasticizer is less hindered in the PAN-based polymer electrolytes, the increase in ionic conductivity at 0–10 °C by melting of the crystal is more prominent.
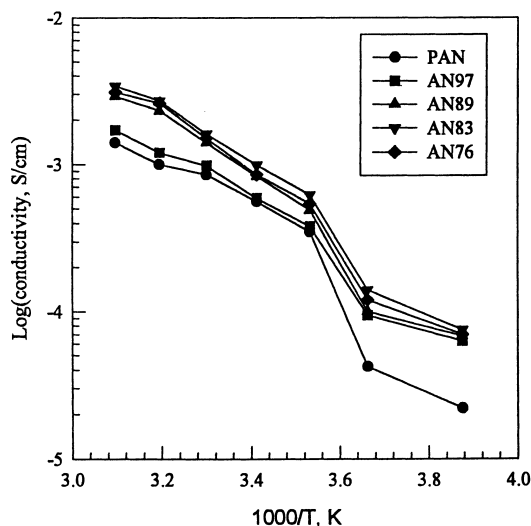
Fig. 5 Arrhenius plot of the ionic conductivies for the polymer electrolytes based on PAN and P(AN-*co*-MMA)

Fig. 6 Complex impedance diagrams for the Li/polymer electrolytes/Li cells prepared with PAN and AN89

The ionic conductivities of the polymer electrolytes prepared with the copolymers of various composition were in the range 8.6×10^{-4} –1.6×10^{-3} S/cm. The observed ionic conductivity of the PAN-based polymer electrolyte was found to be a little lower than those of the copolymer-based polymer electrolytes. At first glance, this result conflicts with the existence of the microchannel in the PAN-based polymer electrolytes, where the physical state of the plasticizer is similar to that of the pure plasticizer: with increasing the fraction of the AN unit in the copolymer, a less amount of the polymer would be involved in the plasticizer-rich phase, and thus the microviscosity of the conducting medium should be decreased and thus result in an increase in ionic conductivity [8]. However, it should be noted that for the phase-separated polymer electrolytes the ionic conductivity calculated from the resistance determined by the impedance measurements could not mean the real ionic conductivity of the conducting medium [23]. In the case that microphase separation occurs, the electrode should be interfaced partly with the PAN-rich phase and also partly with the plasticizer-rich phase, and the PAN-rich phase contributes little to ionic conduction. Therefore, the effective contact area between the plasticizer-rich phase and the electrode should be smaller than the area of the electrode, resulting in lower ionic conductivity for the PAN-based polymer electrolytes compared with the copolymer-based polymer electrolytes.

Interfacial resistance between Li electrode and the polymer electrolytes

Besides high ionic conductivity, low passivation at the Li/electrolyte interface is also required for practical application of the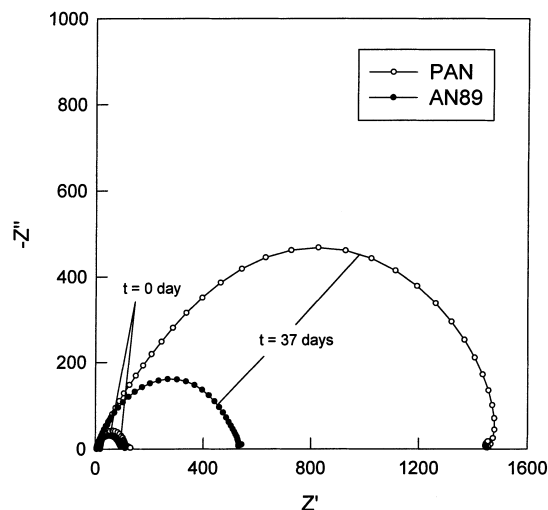 polymer electrolytes. For the investiga-tion of the stability of the Li interface in electrolytes cells, impedance spectroscopy was used. Accordingly, evaluation of the interface characteristics has been carried out by monitoring the time evolution of the a.c. impedance of the symmetric cell (Li/polymer electrolytes/Li) at room temperature. Figure 6 shows the complex impedance responses of the two Li/polymer electrolyte/Li cells prepared with PAN and AN89, respectively. The diameter of the semicircle found in Fig. 6 corresponds to the interfacial resistance, which is known to be caused by the formation of the passivation layer on the Li electrode by reaction between the plasticizer and the Li electrode. The middle frequency semicircle progressively expands after storage at room temperature. This expansion means an increase of the interfacial resistance and may quite likely be associated with a continuous growth of the passivation layer, the product of the corrosion reaction of the Li in the electrolyte medium [15]. In the comparison of the interfacial resistance after 37 days of storage, AN89 showed much lower interfacial resistance than PAN. This suggests that the formation of the passivation layer is suppressed by the incorporation of the MMA unit into the polyacrylonitrile chain.

Figure 7 represents the time evolution of the interfacial resistance for the PAN- and AN89-based polymer electrolytes. The interfacial resistance was found to be initially stable but it was abruptly increased at a certain storage time. This may indicate that the nature of the Li passivation process progressively changes during the contact of the polymer electrolyte with the electrode. The PAN-based polymer electrolyte showed a much larger increase in the interfacial resistance during storage than the AN89-based polymer electrolyte. These results demonstrate the merit of the copolymer over PAN as a matrix polymer for prolonged use in Li rechargable batteries. In the present state, we regard this behavior as
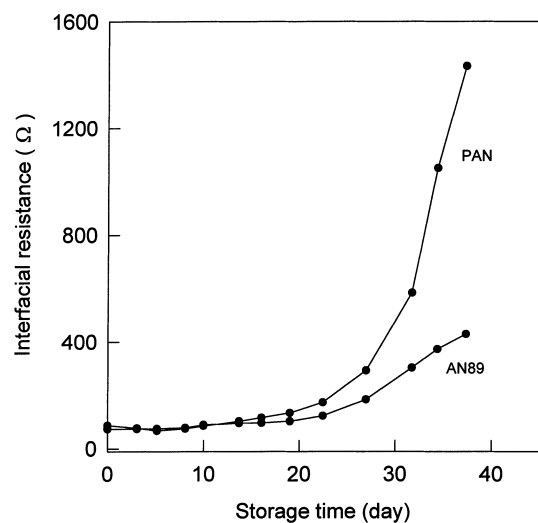
Fig. 7 Time evolution of interfacial resistance of the PAN-based polymer electrolyte and the AN89-based polymer electrolyte

such that the MMA unit introduced into the polyacrylonitrile chain enhances the miscibility between host polymer and plasticizer and provides good adhesion of the polymer electrolyte to the electrode. The difference in the mechanical state of the plasticizer seems to support this consideration. However, the reason for the high increase of the interfacial resistance at relatively long storage times is still unclear. More detailed studies on the interfacial behavior for P(AN-co-MMA) in contact with the electrode is now under progress in our laboratory.

References

1. Croce F, Gerace F, Dautzemberg G, Passerini S, Appetecchi GB, Scrosati B (1994) Electrochem Acta 39: 2187
2. Peramunage D, Pasquariello DM, Abraham KM (1995) J Electrochem Soc 142: 1789
3. Huang B, Wang S, Huang X, Xue R, Chen L (1997) J Electrochim Soc 144: 44
4. Starkey SR, Frech R (1997) Electrochim Acta 42: 471
5. Abraham KM (1993) Electrochim Acta 38: 1233
6. Doeff MM Visco SJ, Ma Y, Peng M, Ding L, DeJonhe LC (1995) Electrochim Acta 40: 2205
7. Peled E, Golodnitsky D, Ardel G, Eshkenazt V (1995) Electrochim Acta 40: 2197
8. Watanabe M, Kanba M, Nagaoka K, Shinohara I (1983) J Polym Sci Polym Phys Ed 21: 939
9. Tsunemi K, Ohno H, Tsuchida E (1983) Electrochim Acta 28: 591
10. Tsunemi K, Ohno H, Tsuchida E (1983) Electrochim Acta 28: 833
11. Alamgir M, Abraham KM (1993) J Electrochem Soc 140: L96
12. Passerini S, Rosolen JM, Scrosati B (1993) J Power Sources 45: 333
13. Hong H, Liquan C, Xuejie H, Rongjian X (1992) Electrochim Acta 37: 1671
14. Surampudi S, Shen DH, Huang C-K, Narayanan SR, Attia A, Halpert G, Peled E (1996) J Power Sources 43–44, 21
15. Groce F, Scrosati B (1993) J Power Sources 43–44, 9
16. Christie AM, Lisowska-Oleksiak A, Vincent CA (1995) Electrochim Acta 40: 2405
17. Croce F, Scrosati B (1993) J Power Sources 44: 9
18. Abraham M, Alamgir M (1993) J Power Sources 44: 195
19. Appetecchi B, Groce F, Scrosati B (1995) Electrochim Acta 40: 8
20. Tonelli AE (1989) NMR spectroscopy and polymer microstructure. AT&T Bell Laboratories Murray Hill NJ
21. Ohno H, Hisatani K, Kamide K (1993) K Polymer J 25: 245
22. Kim CH, Kim HT, Park JK, Moon SI, Yoon MS (1996) J Polym Sci Polym Phys Ed 34: 2709
23. Kim CH, Kim HT, Park JK (1996) J Appl Polym Sci 60: 1773